International Journal of Remote Sensing
Vol. 27, No. 21, 10 November 2006, 4819–4838

Taylor & Francis
Taylor & Francis Group

SRTM vs ASTER elevation products. Comparison for two regions in Crete, Greece

K. G. NIKOLAKOPOULOS†, E. K. KAMARATAKIS‡ and N. CHRYSOULAKIS*§

†University of Athens, Department of Geology and Geoenvironment, Remote Sensing Laboratory, Iroon Polytechniou Str. 15127, Melissia, Greece
‡University of Leicester, Department of Geography, Leicester LE1 7RH, UK
§Foundation for Research and Technology, Hellas, Institute of Applied and Computational Mathematics, Vassilika Vouton, PO Box 1527, GR-71110, Heraklion, Crete, Greece

(*Received 7 November 2005; in final form 5 January 2006*)

The Shuttle Radar Topography Mission (SRTM) collected elevation data over 80% of earth's land area during an 11-day Space Shuttle mission. With a horizontal resolution of 3 arc sec, SRTM represents the best quality, freely available digital elevation models (DEMs) worldwide. Since the SRTM elevation data are unedited, they contain occasional voids, or gaps, where the terrain lay in the radar beam's shadow or in areas of extremely low radar backscatter, such as sea, dams, lakes and virtually any water-covered surface. In contrast to the short duration of the SRTM mission, the ongoing Advanced Spaceborne Thermal Emission and Reflection Radiometer (ASTER) is continuously collecting elevation information with a horizontal resolution of 15 m. In this paper we compared DEM products created from SRTM data with respective products created from ASTER stereo-pairs. The study areas were located in Crete, Greece. Absolute DEMs produced photogrammetricaly from ASTER using differentially corrected GPS measurements provided the benchmark to infer vertical and planimetric accuracy of the 3 arc sec finished SRTM product. Spatial filters were used to detect and remove the voids, as well as to interpolate the missing values in DEMs. Comparison between SRTM- and ASTER-derived DEMs allowed a qualitative assessment of the horizontal and vertical component of the error, while statistical measures were used to estimate their vertical accuracy. Elevation difference between SRTM and ASTER products was evaluated using the root mean square error (RMSE), which was found to be less than 50 m.

1. Introduction

The vast majority of social and environmental processes are global in scope; therefore the study of such processes requires global datasets (Shortridge and Goodchild 1999). Global elevation datasets are inevitably subjected to errors, mainly due to the methodology followed to extract elevation information and the various processing steps the models have undergone (e.g interpolation). Extensive and systematic evaluation of such datasets is difficult due to lack of substantial ground truthing. The past few decades, many efforts to assembly global elevation

*Corresponding author. Email: zedd2@iacm.forth.gr

International Journal of Remote Sensing
ISSN 0143-1161 print/ISSN 1366-5901 online
http://www.tandf.co.uk/journals
DOI: 10.1080/01431160600835853

datasets have been undertaken. In 1986, SPOT was the first satellite to provide stereoscopic images that allowed extraction of DEMs over large areas of the Earth's surface. For the first time, the scientific community were able to extract three-dimensional data over areas of interest that were still inaccessible before SPOT launch. Since this time, various analogue or digital sensors in the visible spectrum have been flown, providing users with spatial data for extracting and interpreting three-dimensional information on the Earth's surface. During the early years the satellite stereo-pairs were acquired across track on different days (SPOT, ERS etc.). More recently, the same-date, along-track stereo-data acquisition was adopted on the ASTER radiometer onboard the Terra satellite. It reduces the radiometric image variations (refractive effects, sun illumination, temporal changes) and thus increases the correlation success rate in any image matching. The automatic DEM generation has become an important part of international research in the last 10 years as a result of the existence of many satellite sensors that can provide stereo pairs. Many new algorithms have been developed, the performances of which have been assessed and reported in the literature (Zhen *et al*. 2001, Toutin *et al*. 2001, Lee *et al*. 2003, Toutin 2001, 2004).

Another commonly used method for extracting relative or absolute elevation information is radar interferometry, or InSAR if a synthetic aperture radar (SAR) is used. It presents the main advantages of radar systems and of digital image processing: all-weather, night and day operation, and automated or semi-automated processing. The necessary data can be collected either by the same antenna during two different passes (Earth Resources Satellites 1 and 2), or by two antennas during the same pass (Shuttle Radar Topography Mission, SRTM). The phase difference information between the SAR images is used to measure precisely changes in the range, on the subwavelength scale, for corresponding points in an image pair. Analysis of the differential phase, and therefore change in distance, between the corresponding pixel centres and the observing antenna can lead to information on terrain elevation (Li and Goldstein, 1990, Gabriel and Goldstein, 1988).

If the SAR data are acquired from the same antenna during two different passes, the imaging geometry of the first pass must be repeated almost exactly in the second pass. The concept of the critical baseline was introduced (Gabriel and Goldstein 1988, Massonnet and Rabaute 1993) to describe the maximum separation of the satellite orbits in the direction orthogonal to both the along-track direction and the radar range direction. The SRTM mission (Werner 2001, Rosen *et al*. 2001) was the first mission using space-borne single-pass interferometric SAR. This mission was a partnership between NASA and the Department of Defense's National Imagery and Mapping Agency (NIMA). In addition, the German and Italian space agencies contributed an experimental high-resolution imaging radar system. Flown aboard the NASA Space Shuttle Endeavour on 11–22 February 2000, the SRTM successfully collected data over 80% of the Earth's land surface, for most of the area between 60° N and 56° S latitude. The heart of the SRTM radar was the Spaceborne Imaging Radar-C/X-band Synthetic Aperture Radar (SIR-C/X-SAR), which flew twice on the Space Shuttle in 1994. Several modifications were made, which gave the SRTM system new capabilities compared with the SIR-C/X-SAR. The major changes were the addition of C-band and X-band antennas at the end of a 60 m mast. These secondary, or "outboard" antennas, allowed the radar to use interferometry to map the elevation of the terrain in a single pass, which was not possible with SIR-C/X-SAR. The American C-band system SIR-C operated with a

wavelength of $\lambda = 5.6$ cm; the wavelength of the German/Italian X-band system was $\lambda = 3.1$ cm. In order to obtain a global coverage between 60° north and 58° south the Shuttle was flown at an altitude of 233 km with an inclination of 57°.

The SRTM DEM products are being distributed mainly under two forms; these are the SRTM 1″ and SRTM 3″, with spatial resolution of 1 and 3 arc sec, respectively. The first is available only for the USA, while the latter is freely distributed for the rest of the globe. Both datasets can be downloaded from various data gateways; one is the USGS seamless data distribution website (USGS 2005). Although currently many applications use SRTM products around the world, there is limited scientific literature on their quality and application fitness. According to mission specifications (Hensley *et al.* 2001), SRTM was expected to generate DEMs with a vertical RMSE of 16 m. The equivalent vertical accuracy requirements for topographic data at scale 1 : 250,000 that meet the USA map accuracy standards (Welch and Marko 1981, Lang and Welch 1999) indicate that RMSE should be around 15.3 m.

The Advanced Spaceborne Thermal Emission and Reflection Radiometer (ASTER) is an advanced multispectral imager that was launched on board NASA's Terra spacecraft in December, 1999. Its viewing geometry is suitable for DEM generation with horizontal spatial resolution of 15 m and a near-pixel-size vertical accuracy. ASTER consists of three separate instruments subsystems, each operating in a different spectral region, using separate optical system. The visible–near infrared system, which is used in DEM production, consists of two telescopes—one nadir looking with a three-band detector and the other backward looking (27.7° off-nadir) with a single band detector. The most important specifications of the ASTER stereo subsystem that govern the DEM generation capabilities include: stereo geometry; platform altitude of 705 km and base-to-height ratio of 0.6 (Abrams 2000).The ASTER stereo-imaging has a relatively modest base-to-height ratio, the disadvantages of which are more than compensated for by the relative radiometric uniformity and freedom from temporal change offered by the forward-nadir stereo geometry. The viability of stereo correlation for parallax difference from digital stereoscopic data has been described and evaluated in previous studies (Al-Rousan and Petrie 1998, Lang and Welch 1999). ASTER DEM data provided the first high-resolution near-global elevation source. Although this remarkable data set is extremely useful due to its relatively high resolution, it suffers from some drawbacks, such as the lack of coverage in several areas due to the weather conditions during the stereo-imagery acquisition.

Error in elevation data is widely recognized to comprise mainly two components, the horizontal, often referred as positional accuracy, and the vertical component or accuracy of the attribute. However, positional and attribute accuracy generally cannot be separated; the error may be due to an incorrect elevation value at the correct location, or a correct elevation for an incorrect location or some combination of these. In this paper SRTM- and ASTER-derived DEMs for two regions in Crete (North Heraklion and Sitia) were compared. Masks and filters were applied to the DEMs to detect and remove the possible voids, to interpolate the missing values and to separate the land from the sea. The vertical error of a 3″ SRTM product was therefore evaluated using a higher accuracy DEM product. This reference DEM was produced by applying a digital stereo correlation approach to ASTER stereo pairs. Ground trouthing was provided by GCP's (ground control points) derived from GPS (global positioning system) measurements differentially

corrected using the GPS base station of the Foundation for Research and Technology, Hellas (Chrysoulakis *et al*. 2004).

2. Data and methodology

2.1 *Study area*

The study focuses in two regions in the island of Crete as shown in figure 1: North Heraklion and Sitia. North Heraklion is located at the central part of Crete and covers an area approximately 70 by 50 km. The topography of the area includes parts of the two most significant mountains of the island, mountain ''Idi'' on the left and ''Dikti'' on the right. The central part of the area is characterized by moderate to high relief with an elevation range of 700 m, while elevation at the two above-mentioned mountains exceeds the value of 2000 m. In the northwest part of the area, an extensive hydrological network consisting of multiple watersheds and channels exists. The area of Sitia is located at the Eastern most part of the island; it covers an area approximately 50 by 40 km. It is a mountainous area characterized by high relief which extents to the coastline; the elevation exceeds 1500 m. Series of hydrological channels leading to the north and south cost exist. These regions were chosen because of their limited voids—''no data pixels'' in both datasets—and the availability of the ASTER stereo pairs and GCPs.

2.2 *Data preparation*

SRTM elevation data was obtained from the GLCF (Global Land Cover Facility) of the University of Maryland (GLCF 2005). The GLCF provides SRTM data in Geotiff format after a short processing and at three horizontal resolutions:

- 1 arc sec/30 m DEM of the USA;
- 3 arc sec/90 m DEM of the world;

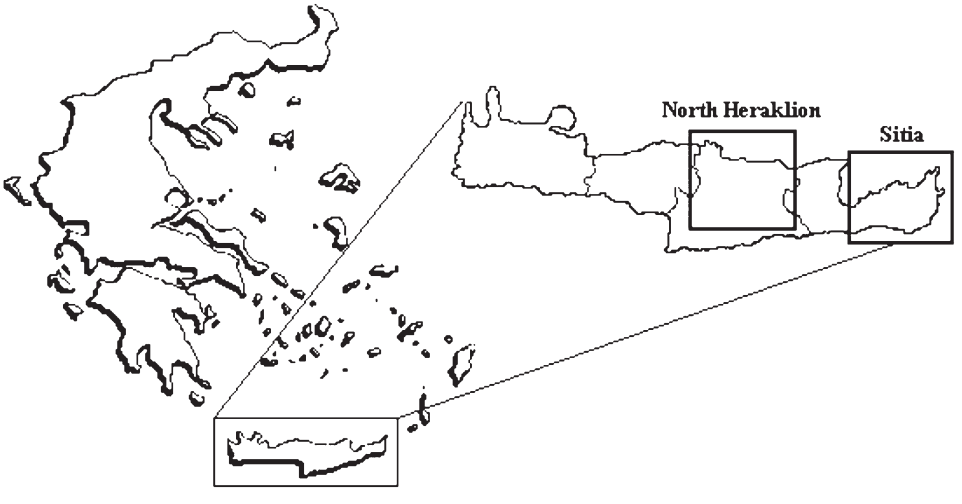

Figure 1. The study area.

- 30 arc sec/1 km SRTM-GTOPO30 product corrected by GTOPO30 30 arc sec DEM.

All studies employing DEMs make use of planar coordinates to have the same measurement units for both (x, y) and elevation. The SRTM data were provided in UTM WGS84, therefore it was necessary to reproject the SRTM-derived DEM to the Hellenic Geodetic Reference System 87 (HGRS87), because the reference ASTER DEM was produced with respect to that grid. When dealing with multiresolution datasets, there is often a need for data sampled at one scale to be generalized to other scales. In this study, we had to compare two elevation datasets sampled at different scales (spatial resolutions). The pixel size of the ASTER-derived DEM was 15 m, whereas the SRTM-derived DEM had a pixel dimension of 90 m, as provided by the GLCF. In order to compare the two datasets, the ASTER DEM was scaled up to an aggregated pixel size, matching the dimensions of the SRTM grid.

The SRTM-derived elevation data used in this study were initially referenced to the WGS84 EGM96 geoid, and horizontally georeferenced to the WGS-84 ellipsoid using a UTM projection. The values so measured could correspond to the bare earth, the top of the vegetation, or the top of man-made features. The minimum value (representing the voids) was −32,768 and the maximum value was 2433. The original SRTM elevation data were reprojected to the HGRS 87 using the nearest neighbourhood resampling method and preserving the 90 m pixel size. The nearest neighbour resampling method was used to preserve the values of the DEM and particularly the voids. Then, a spatial filter was applied to the SRTM DEM. This filter detected all the negative values and changed them to the value −5, resulting a DEM with less noise and homogenous voids. The borderline of the two study areas was used to create binary masks to separate the land from the sea. It should be noted that the SRTM DEM contained many more voids in the Sitia area (with a quite large extent that exceeded in some cases 0.75 km^2) than in the North Heraklion area. Especially in the western part of the Sitia area, there were many large voids with a NNE–SSW orientatopm. This may be explained by the NNE–SSW orientation of the high mountains in this area. Following this, a second spatial filter was applied to both DEMs to interpolate the missing values. The filter initially detected the areas with the specified value of −5. If the majority of the pixels around this area had to be replaced, then a low pass filter 5×5 was applied; otherwise a low-pass 3×3 filter was applied.

The ASTER-derived DEMs used in this study were produced in the framework of the REALDEMS project, aiming at providing accurate DEMs and land cover maps for some Greek islands that were capable of being used in local studies. As a part of this project, high spatial resolution ASTER stereo imagery was analysed to produce DEM for Heraklion and Sitia areas. Differentially corrected GPS measurements were performed to provide GCPs for DEM correction and geo-location. The planimetric and elevation accuracies (RMSE resulting from using survey monuments available from 1 : 5000 survey maps) of the produced DEMs were 15.0 and 12.4 m, respectively. The ASTER DEM production procedure has been described in detail by Chrysoulakis *et al.* (2003, 2004). The DEM for North Heraklion was produced using a single ASTER scene, whereas the DEM for Sitia was produced using a block of two ASTER scenes. As already mentioned, the ASTER-derived DEM for both areas was scaled up to an aggregated pixel size matching the dimensions of the SRTM grid.

2.3 *ASTER SRTM DEM comparison*

By superimposing the two DEMs for each area, a noteworthy misalignment of the SRTM DEM was observed, which had probably been caused by the datum transformation process and in particular when the borderline of the two study areas was used to create binary masks to separate the land from the sea. In order to evaluate misalignment, several elevation profiles along the north–south and east–west directions for both SRTM and ASTER DEMs were compared. The SRTM DEMs were found to be shifted approximately 200 m easting and 400 m northing, which correspond to 2.2 and 4.4 pixels, respectively. To account for this misalignment, a co-registration methodology was applied. Slope was derived for both ASTER and SRTM datasets and two false coloured images were created for each DEM pair (DEM + slope). The texture introduced from slope allowed the location of several control points for an image-to-image co-registration, and thus SRTM DEM was re-registered to ASTER DEM. Following the re-registration, the spatial distribution of elevation difference between two SRTM and ASTER DEMs for both study areas was produced by subtracting the respective images pixel-by-pixel. Since the ASTER DEM is considered as the reference DEM, the difference image also represents an error map for SRTM-derived elevations. Scatter plots of SRTM–ASTER DEM difference vs elevation, as well as vs slope, were used in the comparison procedure.

In order to describe and compare the elevation distributions in each DEM, several descriptive statistic measures were employed, among them skewness and kurtosis (King and Julstrom 1982). Skewness is a unitless measure of asymmetry in a distribution (Shaw and Wheeler 1985). Positive skewness indicates a longer tail to the right, while negative skewness indicates a longer tail to the left. A perfectly symmetric distribution, like the normal distribution, has skewness equal to 0. Excess kurtosis is a unitless measure of how sharp the data peak is. Traditionally the value of this coefficient is compared with a value of 0.0, which is the coefficient of kurtosis for a normal distribution. A value larger than 0 indicates a peaked distribution, while a value less than 0 indicates a flat distribution.

Since both ASTER- and SRTM-derived elevation distributions were close to normal, the *F*-ratio test was applied in order to test against the null hypothesis that the variances of the two DEMs were equal. Two sample *F*-tests for variances of ASTER and SRTM DEMs and the respective slope distributions for both North Heraklion and Sitia were performed and the null hypothesis was rejected in all cases. Therefore, two-sample *t*-tests assuming unequal variances for the means of ASTER and SRTM DEMs and the respective slope distributions for both study areas were performed and the null hypothesis was rejected again in all cases. The null hypothesis in the *t*-tests assumed equal means for the two samples. Moreover, the Kolmogorov–Smirnov nonparametric test that does not use any distributional assumptions was used to check the null hypothesis that the distributions are identical for the two datasets.

To obtain the degree of relationship between the ASTER and SRTM DEMs, Pearson and Spearman correlation coefficients were calculated, for the elevations as well as for the slope derived from them. Pearson's correlation coefficient represents the association between two variables or the degree of co-variation of the two variables or the tendency of variable to vary together in the sense that one increases as the other increases (positive covariation) or in the sense that one variable increases as the other decreases (negative covariation).

The correlation between SRTM- and ASTER-derived elevation values was estimated by analysing the respective scatter plots. Additional, a common measure of quantifying vertical accuracy in DEMs, the root mean square error (RMSE) was used. RMSE is an overall error indicator that takes into account both random and systematic errors introduced during the data generation process. It is currently widely adopted mostly because it is a comprehensive statistic and because it is easy to implement. RMSE is the method adopted by the USGS in order to assess DEM products, comparing them with elevation points that reflect the "most probable" elevations at specific locations. In this study, the RMSE of SRTM DEM in relation to a reference DEM (ASTER DEM) was calculated. The elevation of each SRTM DEM pixel was compared with the elevation of the respective ASTER DEM pixel and the RMSE was calculated directly from raster data by employing an in-house developed spatial model.

The comparisons were made using all valid height and slope values from the SRTM and ASTER sources. The huge amount of data (259,852 pixels for the case of North Heraklion and 109,807 pixels for the case of Sitia) used in calculations provided evidence of the statistical significance of results (the resulting p-value was less than 0.001 in all cases of F-test, t-test and Spearman and Pearson correlation coefficient calculations). As stated above, the RMSE was used as error measure, although the value of the systematic offset and the extent of the variation separately were calculated from the histogram of the error map for SRTM-derived elevations for both cases of North Heraklion and Sitia.

Moreover, the analysis indicated that there was a spatial correlation in the original ASTER and SRTM datasets which inflated the corresponding correlation coefficient. For this reason, the correlation analysis was performed again based on spatially uncorrelated points. To do this a sub-sample of ASTER and SRTM DEMs was used. The sampling was performed at rate that prevented spatial correlations. The sampling rate was defined by analysing the variograms of ASTER and SRTM DEMs, as well as of the respective slope distributions. The variograms for ASTER, SRTM and ASTER–SRTM difference for North Heraklion are shown in figure 2. The range in which the variograms reach their corresponding sills (that is the range where spatial autocorrelation ceases to exist) was too large to allow for a random sample of a satisfactory size. Nevertheless, one may observe that the rate at which the variograms increase is too low for small distances from the origin. Thus, sub-samples with a minimum distance of 3600 m (40 pixels) between sample points were used and the correlation coefficients were calculated based on these sub-samples.

3. Results

Figure 3 shows the SRTM-derived DEM for the area of Sitia after the application of the first spatial filer. The land was separated from the sea using a binary mask. Areas with black pixels represent the voids. The final SRTM DEM for Sitia after the interpolation with a 5×5 low-pass filter is shown in figure 4. The majority of the pixels with no value have been replaced. There are still two voids at the centre of the image and at the left of the image. The extent of the voids in the original DEM was bigger than 0.75 km^2. In the areas in which the 5×5 low pass filter did not manage to interpolate all the missing values, a 7×7 filter was used to eliminate all voids. In contrast, the 5×5 low-pass filter gave excellent results for the area of North Heraklion.

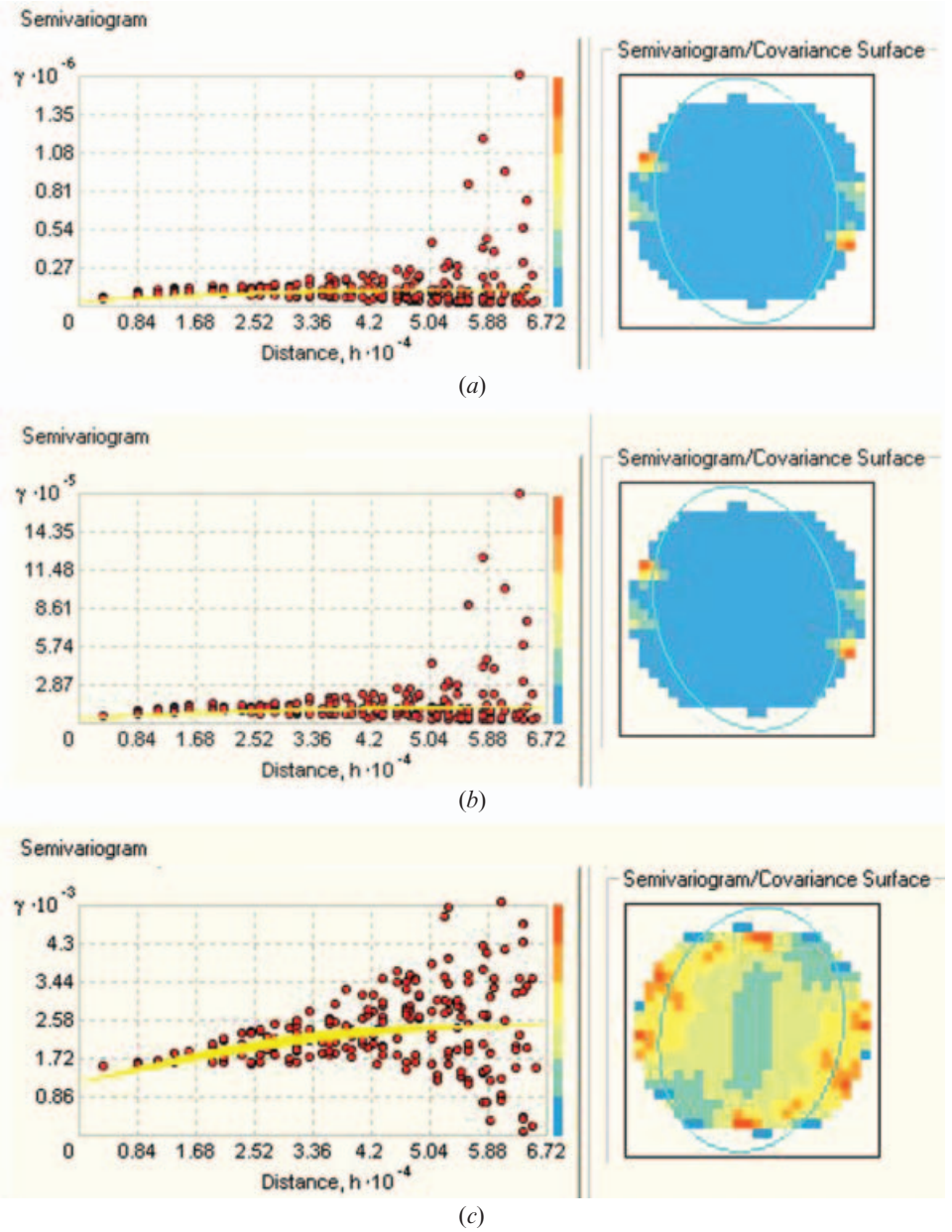

Figure 2. The variograms for ASTER (a), SRTM (b) and ASTER–SRTM difference (c) for North Heraklion. The range where spatial autocorrelation ceases to exist is the range in which the variograms reach their corresponding sills.

Figure 5 shows SRTM DEM before re-registration for both North Heraklion and Sitia areas. One north–south and one east–west elevation profile for each pair of DEMs are also presented. The north–south elevation profile of the SRTM DEM shows a less noisy pattern while the major terrain variations are similar. The patterns do not match exactly due to the misregistration of the SRTM DEM. The misalignment in the north–south direction appears to be approximately 400 m, while

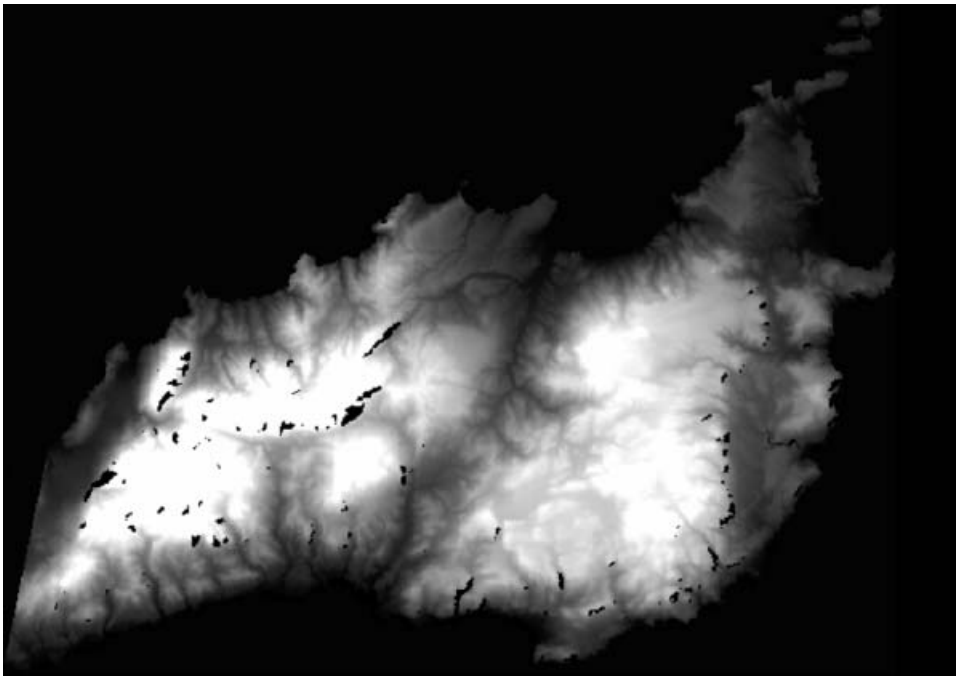

Figure 3. SRTM derived DEM for the area of Sitia after the application of the first spatial filer.

in the east–west direction the misalignment drops approximately to 200 m, corresponding to 4.4 and 2.2 SRTM DEM pixels, respectively.

The re-register SRTM and ASTER DEMs for the area of North Heraklion, as well as their histograms, are presented in figure 6. The frequency histogram of the values for ASTER DEM seems to be noisier while it retains the same overall pattern of the SRTM DEM. The peak values appear in the range 200–400 m in both DEMs. The SRTM DEM contains fewer zero values around the northern coastline. The re-register SRTM and ASTER DEMs for the area of Sitia, as well as their histograms, are presented in figure 7. Several grey value stretches show that the dominant terrain features, large mountains, ridges and troughs are well depicted in both DEMs. This can also be observed from the similarity of the frequency histograms: several peaks in the histograms co-exist in both datasets. This similarity provides evidence that both DEMs give an analogous representation. The major difference in the two histograms occurs at the values around zero. These values represent the elevation values around the coastline. SRTM DEM in the case of Sitia shows a substantially greater amount of near-zero values.

As already mentioned, the *F*-test for variances and *t*-test, assuming unequal variances for the means of ASTER and SRTM DEMs and the respective slope distributions for both study areas, were performed and the null hypotheses were rejected in all cases. Therefore, these tests indicated that the differences between means and variances in ASTER- and SRTM-derived elevations and slopes were statistically significant. The results of the *F*-test for ASTER and SRTM DEMs for North Heraklion are shown in table 1, whereas the respective results of the *t*-test are shown in table 2. The above results were confirmed by a nonparametric test, which does not use any distributional assumptions. The asymptotic *p*-value for the

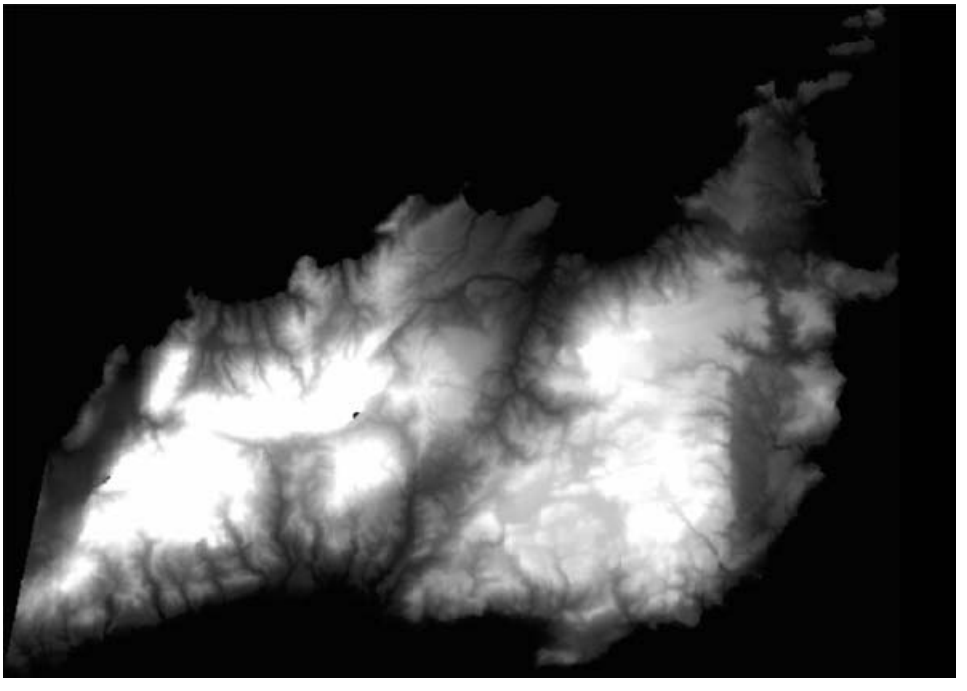

Figure 4. The SRTM DEM for Sitia after the interpolation with a 5×5 low-pass filter. The majority of the pixels with no value have been replaced. There are still two voids at the center of the image and at the left part of the image. The extent of the voids in the original DEM was bigger than 0.75 km^2.

Kolmogorov–Smirnov test for the empirical distribution functions was less than 0.0001. This indicated rejection of the null hypothesis that the distributions are identical for the two datasets.

Table 3 shows the summary statistics for ASTER- and SRTM-derived elevation and slope for both study areas. The difference of the mean value (mean elevation) for the Sitia region is 7.82 m and for the North Heraklion region is 2.36 m. The difference in the max value (higher elevation) is 3 and 29 m for the Sitia and the North Heraklion region, respectively. It appears that the distributions derived from the two DEMs for both study areas are of the same shape regarding symmetry and fat-tailedness since the skewness and kurtosis indices practically coincide. SRTM elevation observations are significantly less dispersed with lower mean values. Thus, although the two distributions are of the same shape, the one derived from SRTM is more condensed and shifted to the left; this is evident for elevation measurements, whereas it holds less strongly as far as slopes are concerned.

The SRTM- and ASTER-derived elevations for both study areas show a substantial strong positive correlation. The results that are depicted in table 4, indicating strong correlation for estimated elevation between the two DEMs; observations corresponding to slope are much smaller, but still positively correlated. Given the sample size, both correlation indices are statistically significant. The correlation for the North Heraklion region is stronger than the correlation for the Sitia region. The scatter plot of SRTM-derived elevation values vs ASTER elevation values for North Heraklion, which are shown in figure 8, reflects this strong correlation.

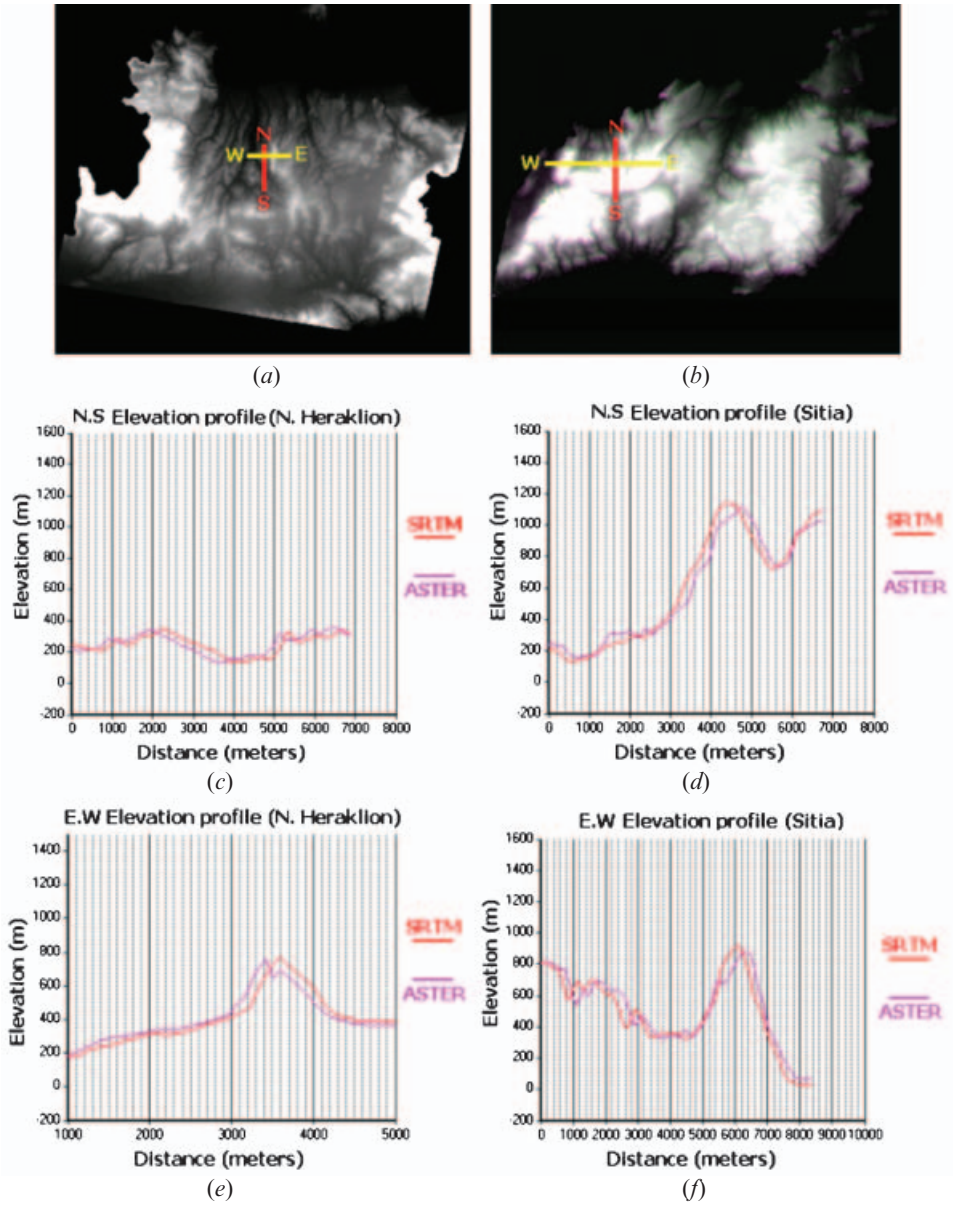

Figure 5. (a) SRTM DEM before re-registration for North Heraklion; (b) SRTM DEM before re-registration for Sitia; (c) north–south elevation profile for North Heraklion; (d) north–south elevation profile for Sitia; (e) east–west elevation profile for North Heraklion; (f) east–west elevation profile for Sitia. The patterns do not match exactly due to the misregistration of the SRTM DEM, the misalignment in the north–south direction appears to be approximately 400 m, while in the east–west direction the misalignment drops approximately to 200 m.

Figure 9 shows the error map for SRTM-derived elevations for the area of North Heraklion. This image was produced by subtracting SRTM elevation values from the ASTER elevation values of the re-registered DEM. From this difference image, it can be observed that most of the high differences occur at the eastern and western

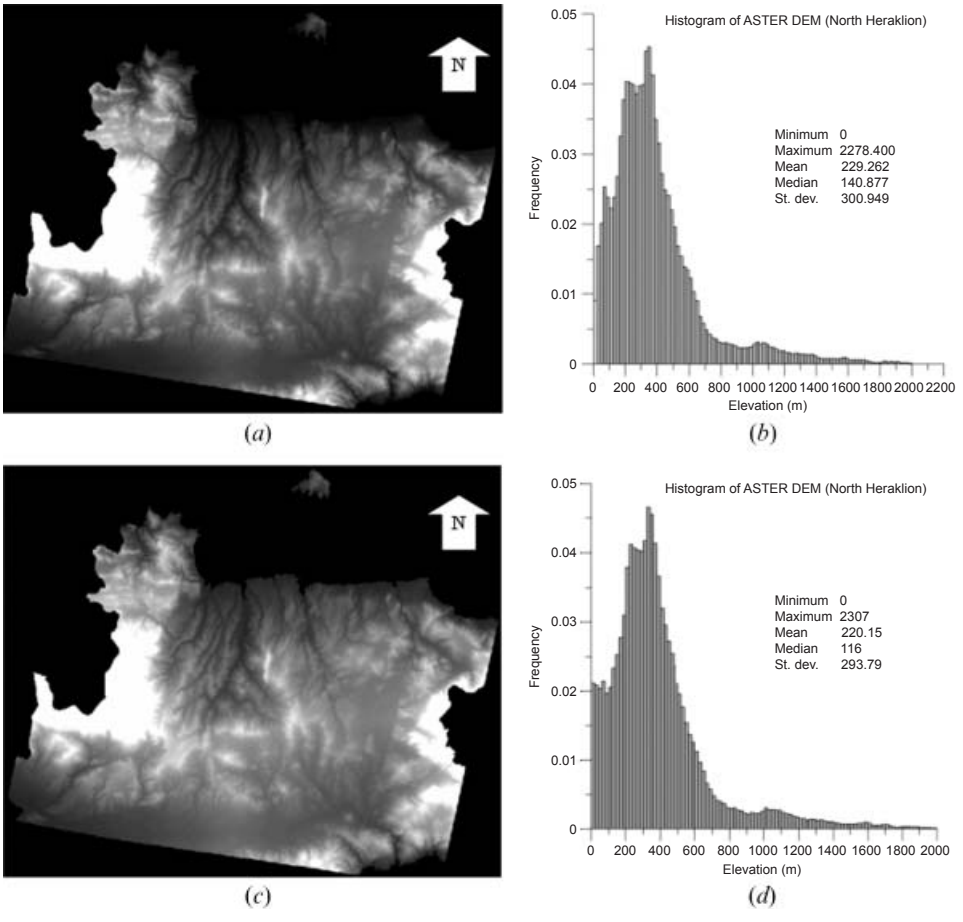

Figure 6. (a) The ASTER-derived DEM for the area of North Heraklion; (b) the ASTER DEM frequency histogram; (c) the re-register SRTM-derived ASTER DEM for the area of North Heraklion; and (d) the SRTM DEM frequency histogram. The two histograms have the same overall pattern and the peak values appear in the range from 200 to 400 m.

borders of the DEMs, where the largest elevation values are (mountains Idi and Dikti). The corresponding frequency histogram is shown in figure 10(a), whereas the histogram corresponding to the error map for the area of Sitia is shown in figure 10(b). These histograms are indicative of the probability distribution of error; the means correspond to biases (systematic effect) and the variances corresponds to random effects; skewness and kurtosis display potential error asymmetries. The respective statistical measures for both histograms are also shown in figure 10. A small positive bias is evident in both histograms indicated that SRTM DEM trends to underestimate the spatial distribution of elevation in both areas. The statistical measures indicate the value of the systematic offset and the extent of the variation separately for both study areas: for North Heraklion the bias is estimated from the mean of the ASTER–SRTM DEM difference (2.36), whereas the extent of the variation is estimated from standard deviation of the ASTER–SRTM DEM difference (44.87). For Sitia, the values of the mean and standard deviation of ASTER–SRTM DEM difference are 7.83 and 44.74, respectively. It is therefore obvious that, since the value of bias is low in both cases, the variation about the

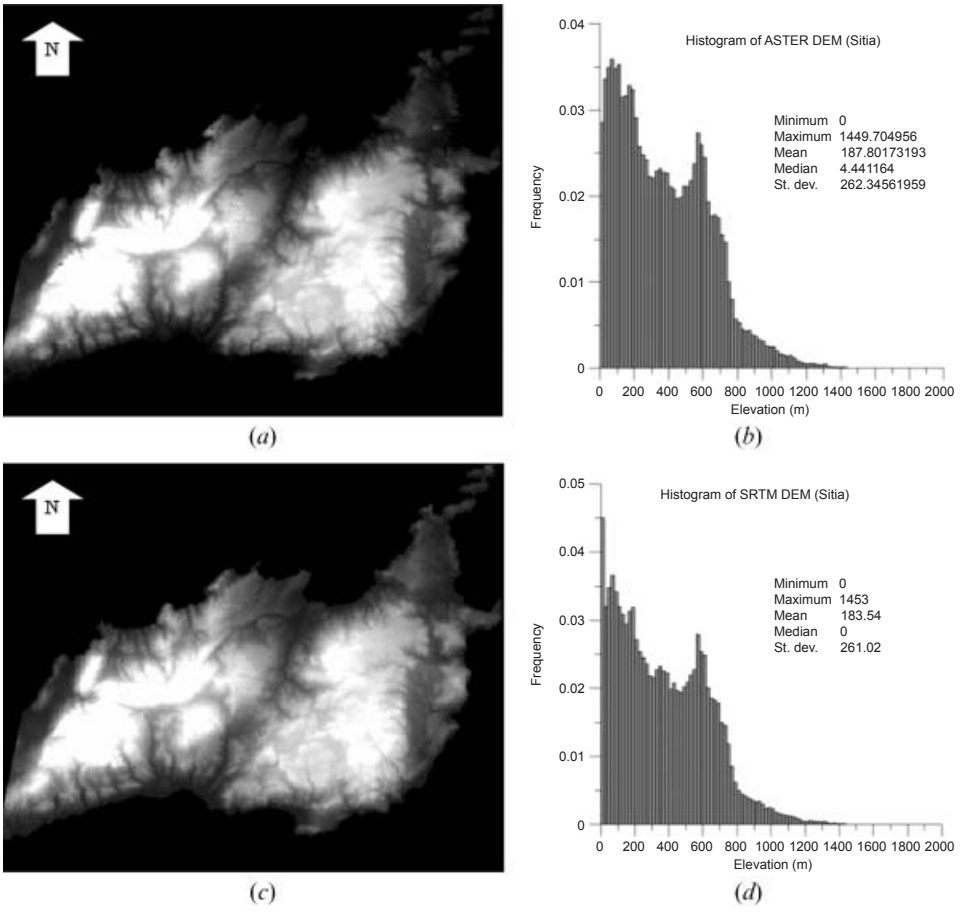

Figure 7. (a) The ASTER-derived DEM for the area of Sitia; (b) the ASTER DEM frequency histogram; (c) the re-register SRTM-derived ASTER DEM for the area of Sitia; (d) the SRTM DEM frequency histogram. The two histograms show that both DEMS give a similar representation, since several peaks coexist in both datasets.

Table 1. Two-sample *F*-test for variances of ASTER and SRTM DEMs for North Heraklion.

Sample statistics				
Group	*N*	Mean	Standard deviation	Variance
1. ASTER DEM	259,851	391.11	297.13	88287.03
2. SRTM DEM	259,851	388.75	294.76	86883.68

Hypothesis test			
Null hypothesis: Variance 1/variance 2=1			
Alternative: Variance 1/variance 2 $\geqslant$ 1			
F	Numerator	Denominator	*P*>*F*
1.02	259851	259851	<0.0001

Table 2. Two-sample *t*-test assuming unequal variances for the means of ASTER and SRTM DEMs for North Heraklion.

Sample statistics				
Group	*N*	Mean	Standard deviation	Standard error
1. ASTER DEM	259,851	391.11	297.13	0.5829
2. SRTM DEM	259,851	388.75	294.76	0.5782

Hypothesis test			
Null hypothesis: Mean 1–mean 2=0 Alternative: Mean 1–mean 2 ⩾ 0			
	t-Statistic	Df	*P*>*t*
	26.810	259,851	<0.0001

mean is the parameter that mainly affects the value of RMSE, which was calculated at a value of 44.94 m for the case of North Heraklion, whereas for the case of Sitia it was calculated at a value of 45.42 m. Both values were considered quite satisfactory for SRTM-derived DEM.

The scatter plot of ASTER–SRTM elevation difference vs elevation, which is shown in figure 11 for North Heraklion, indicates that there is no elevation-caused bias of this difference. Moreover, it indicates that the majority of differences cluster around zero at an elevation range from zero to about 600 m. That is due to the fact most elevation values in the area are in that range. Clustering of the difference is also observed for the elevation ranges from 1000 m to about 1300 m and from 1700 m to about 2000 m.

The correlation analysis using spatially uncorrelated points was based on sub-samples of ASTER and SRTM DEMs and slopes, as described in section 2.3. The selected distance allows for a sample size of 213 sampling points for North Heraklion, with very low spatial autocorrelation. The correlation coefficient for DEM sub-samples was calculated at values of 0.99013 for North Heraklion and 0.98735 for Sitia, indicating strong correlation of the respective elevation datasets. Figure 12 shows the histogram of the difference between ASTER and SRTM DEM sub-sample for North Heraklion. The mean of the ASTER–SRTM difference of the

Table 3. Summary statistics for SRTM and ASTER derived elevation and slope for both study areas.

Statistic measures		Minimum	Maximum	Mean	Standard deviation	Skewness	Kurtosis
			North Heraklion				
ASTER	Elevation	0	2278	391.11	297.13	2.0487	8.5896
	Slope	1	85	10.78	10.22	2.998	17.401
SRTM	Elevation	0	2307	388.75	294.76	2.0224	8.6957
	Slope	1	85	10.66	10.32	2.9308	16.781
				sitia			
ASTER	Elevation	0	1450	372.31	260.02	0.62831	2.9081
	Slope	1	68	12.10	8.40	1.1465	4.8287
SRTM	Elevation	0	1453	364.49	262.93	0.59848	2.8201
	Slope	1	67	11.94	8.48	1.0331	4.2556

Table 4. Pearson and Spearman correlation coefficients for SRTM- and ASTER-derived elevation and slope for both study areas.

Correlation measures	Elevation		Slope	
	North Heraklion	Sitia	North Heraklion	Sitia
Pearson	0.98854	0.98542	0.81982	0.63511
Spearman	0.97840	0.98295	0.68864	0.60826

sub-sample obtained a value of 0.1, whereas the standard deviation was 45.98. It is therefore obvious that, since the value of bias is low, the variation about the mean is the parameter that mainly affects the RMSE value of the sub-sample, which was calculated at 45.87. This value is close to the value calculated using all valid elevation values (44.94).

4. Conclusions

The goal of this paper was to compare DEMs derived from the SRTM and ASTER data as those two projects have the same purpose: to cover 80% of the Earth's surface with accurate elevation data. For this comparison two areas in the island of Crete were selected. These two areas present a complex physiography with an

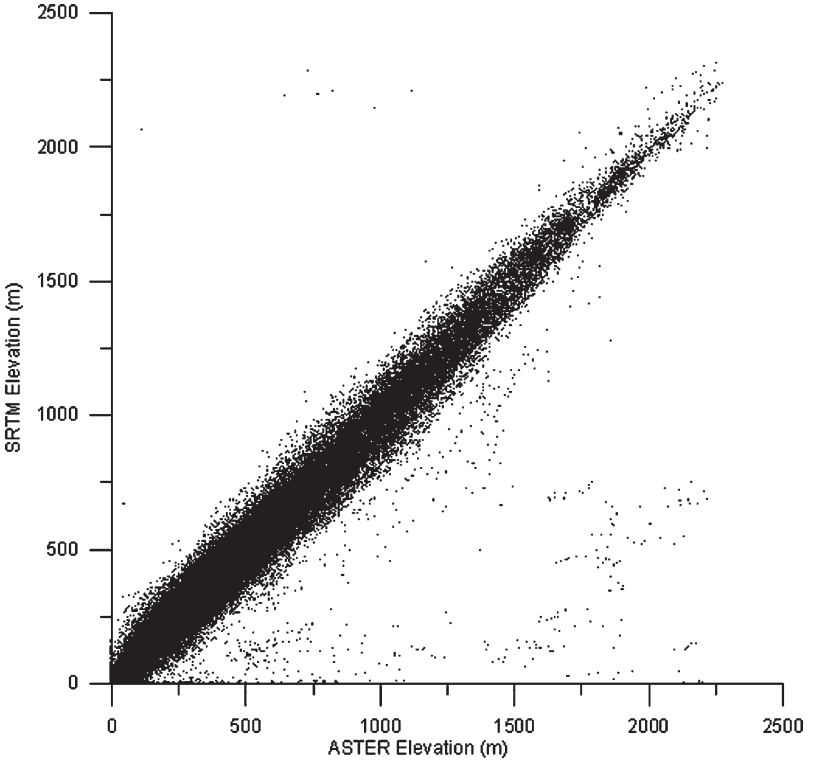

Figure 8. Scatter plot of SRTM derived elevation vs ASTER-derived elevation for North Heraklion. A strong positive correlation can be observed.

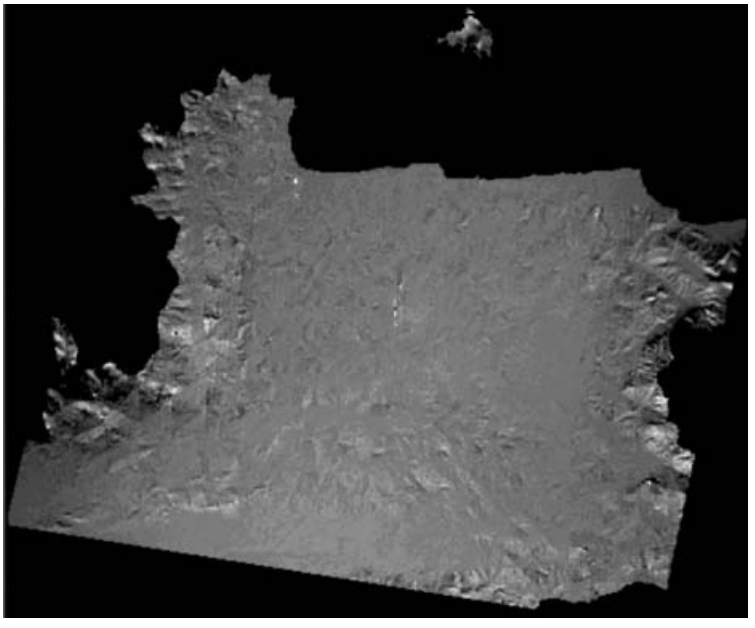

Figure 9. SRTM error map: spatial distribution of ASTER–SRTM elevation values for the area of North Heraklion.

extensive drainage network and elevations that range from 0 to more than 2200 m, and thus those areas are ideal places for DEM accuracy comparison.

The first optical control shows that the two DEMs present much shape similarity, but also a noteworthy displacement. The SRTM DEMs were found to be shifted approximately 200 m easting and 400 m northing, corresponding to 4.4 and 2.2 SRTM DEM pixels, respectively. To account for this misalignment, a co-registration methodology was applied. After re-registration of SRTM DEMs, a similarity of their frequency histograms with the respective ASTER DEM histograms was observed, providing evidence that both DEMS give an analogous representation of the Earth's surface.

Error maps for SRTM-derived elevations for both study areas was produced by subtracting SRTM elevation values from the respective ASTER values. The difference of the mean value (mean elevation) for the Sitia region is 7.82 m and for the North Heraklion region is 2.36 m. The mean value of the difference is close to near-zero negative values. The corresponding frequency histograms indicated that the SRTM elevation was slightly underestimated.

Comparison between SRTM and ASTER derived DEMs allowed a qualitative assessment of the horizontal and vertical component of the error, while statistical measures were used to estimate their vertical accuracy. Skewness and kurtosis were used to compare the frequency histograms of the elevation distributions in both DEMs in each study area. The elevation distributions derived from the two DEMs for both study areas were of the same shape regarding symmetry and fat-tailedness. Scatter plots, as well as Pearson and Spearman correlation coefficients, were used to obtain the degree of relationship between the ASTER and SRTM DEMs. The results indicated strong correlation for estimated elevation between them. The original ASTER and SRTM datasets were spatially correlated. For this reason,

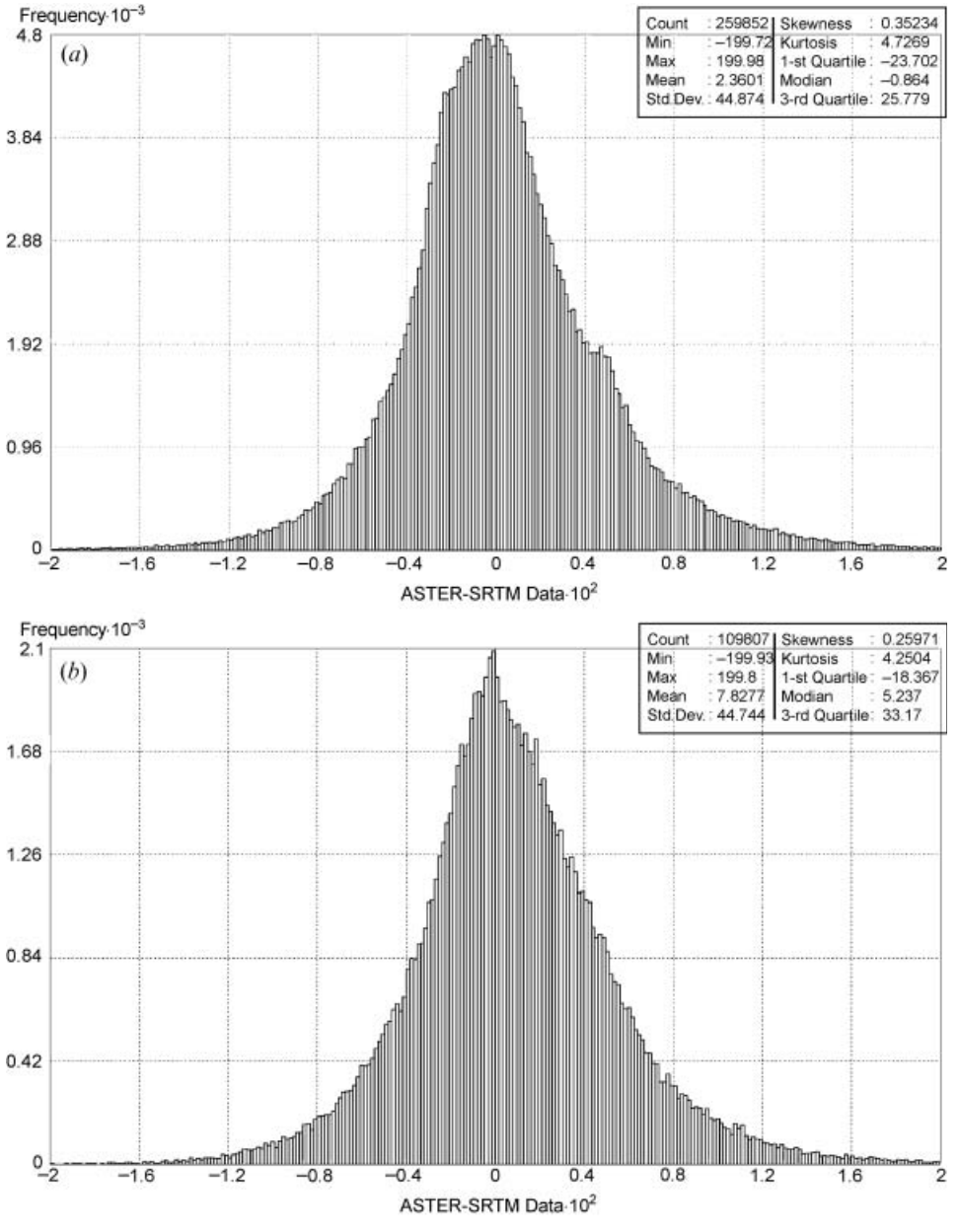

Figure 10. (a) Histogram and statistics of the SRTM error map for North Heraklion; (b) histogram and statistics of the SRTM error map for Sitia. A small positive bias is evident in both histograms.

the correlation procedure was repeated using sub-samples of spatially uncorrelated points. The correlation coefficients corresponding to these sub-samples were high in all cases, indicating a strong correlation of the respective datasets.

The systematic offset and the extent of the variation were calculated for DEMs and slopes in both study areas and, finally, the RMSE was used to evaluate the vertical accuracy of SRTM DEM. The RMSE was calculated at a value of 44.94 m

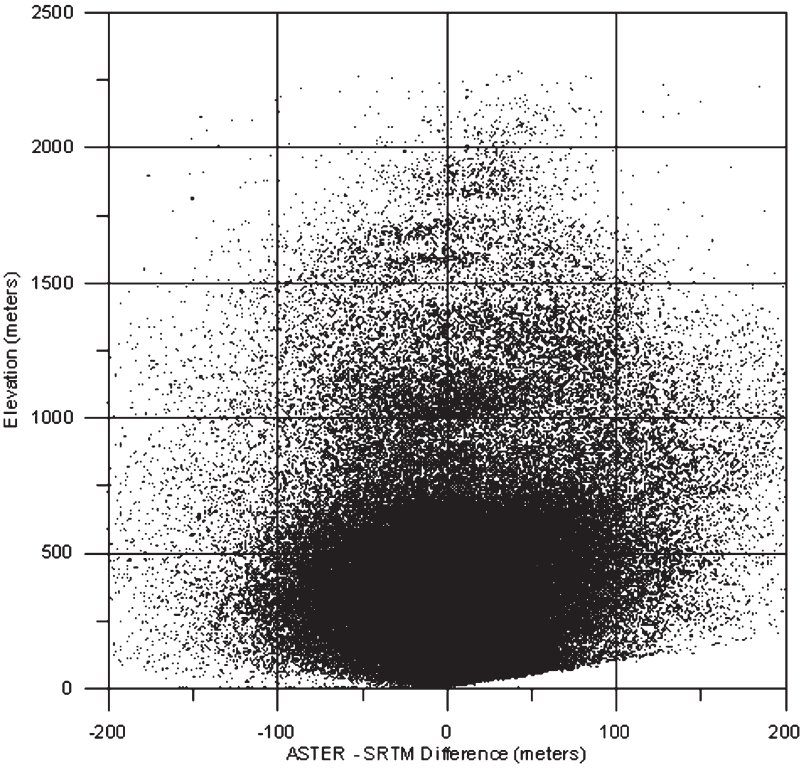

Figure 11. Scatter plot of ASTER–SRTM DEM difference vs elevation for North Heraklion. No important bias can be observed.

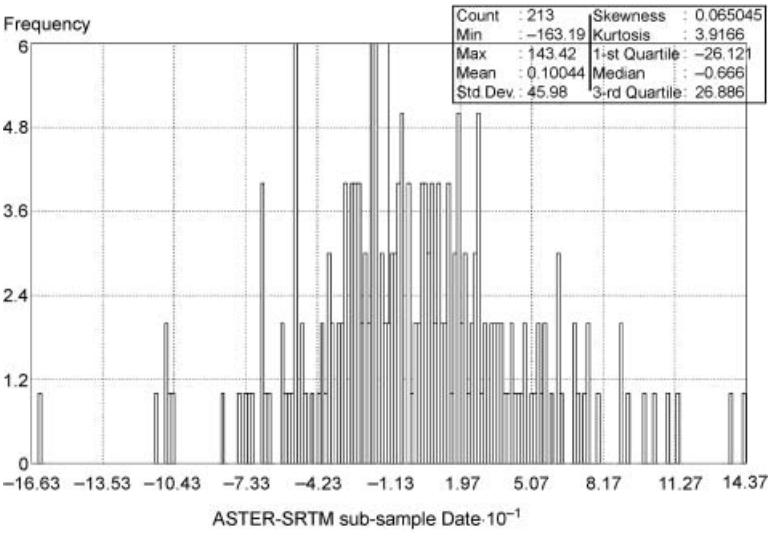

Figure 12. Histogram of the difference between ASTER and SRTM DEM sub-sample for North Heraklion.

for the case of North Heraklion, whereas for the case of Sitia it was calculated at a value of 45.42 m. Both values were considered quite satisfactory for SRTM-derived DEM.

Acknowledgement

The authors are grateful to Y. Kamarianakis (Foundation for Research and Technology, Hellas, Institute of Applied and Computational Mathematics), for statistical analysis support.

References

ABRAMS, M., 2000, ASTER: data products for the high spatial resolution imager on NASA's EOS-AM1 platform. *International Journal of Remote Sensing*, **21**, pp. 847–861.

AL-ROUSAN, N. and PETRIE, G., 1998, System calibration, geometric accuracy testing and validation of DEM and orthoimage data extracted from SPOT stereopairs using commercially available image processing systems. *International Archives of Photogrammetry and Remote Sensing*, **32**, pp. 8–15.

CHRYSOULAKIS, N., DIAMANDAKIS, M. and PRASTACOS, P., 2003, GIS Integration of ASTER stereo imagery for the support of Watershed Management. *Global Nest: The International Journal*, **5**, pp. 47–56.

CHRYSOULAKIS, N., ABRAMS, M., FEIDAS, H. and VELIANITIS, D., 2004, Analysis of ASTER multispectral stereo imagery to produce DEM and land cover databases for Greek islands: the REALDEMS Project. In *Proceedings of e-Environment: Progress and Challege*, P. Prastacos, U. Cortes, J.L. De Leon and M. Murillo (Eds), pp. 411–424 (Mexico: Institute Politecnico National).

GABRIEL, A.K. and GOLDSTEIN, R.M., 1988, Crossed-orbit interferometry: theory and experimental results from SIR-B. *International Journal of Remote Sensing*, **9**, pp. 857–872.

GLCF, 2005, Global Land Cover Facility. Shuttle Radar Topography mission. University of Maryland; http://glcf.umiacs.umd.edu/data/srtm/index.shtml (accessed December 2005).

HENSLEY, S., MUNJY, R. and ROSEN, P., 2001, In *Interferometric Synthetic Aperture Radar (IFSAR), Digital Elevation Model Technologies and Applications: The DEM Users Manual*, D. Maune (Ed.), pp. 143–206 (Bethesda, MD: American Society for Photogrammetry and Remote Sensing).

KING, R.S. and JULSTROM, B., 1982, *Applied Statistics Using the Computer* (Sherman Oaks, CA: Alfred Pub. Co.).

LANG, H. and WELCH, R., 1999, ATBD-AST-08 Algorithm Theoretical Basis Document for ASTER Digital Elevation Models. Standard Product AST14 Report, The Jet Propulsion Laboratory, California Institute of Technology, Los Angeles, CA.

LEE, H.-Y., KIM, T., PARK, W. and LEE, H.-K., 2003, Extraction of digital elevation models from satellite stereo images through stereo matching based on epipolarity and scene geometry. *Image and Vision Computing*, **21**, pp. 789–796.

LI, F. and GOLDSTEIN, R.M., 1990, Studies of multi-baseline spaceborne interferometric synthetic aperture radars. *IEEE Transactions on Geoscience and Remote Sensing*, **28**, pp. 88–97.

MASSONNET, D. and RABAUTE, T., 1993, Radar inteferometry: limits and potential. *IEEE Transactions on Geoscience and Remote Sensing*, **31**, pp. 455–464.

ROSEN, P., EINEDER, M., RABUS, B., GURROLA, E., HENSLEY, S., KNÖPFLE, W., BREIT, H., ROTH, A. and WERNER, M., 2001, SRTM Mission—Cross Comparison of X and C Band Data Properties. *Proceedings of IGARSS*, Sydney, Australia, unpaginated CD-ROM.

SHAW, G. and WHEELER, D., 1985, *Statistical Techniques in Geographical Analysis* (Chichester: Wiley).

SHORTRIDGE, A.M. and GOODCHILD, M.F., 1999, Communicating uncertainty for global data sets. In *International Symposium on Spatial Data Quality*, W. Shi, M.F. Goodchild and P.F. Fisher (Eds), pp. 56–65 (Hong Kong: Hong Kong Polytechnic University).

TOUTIN, Th., 2001, Elevation modelling from satellite VIR data: a review. *International Journal of Remote Sensing*, **22**, pp. 1097–1125.

TOUTIN, Th., 2004, Geometric processing of remote sensing images: models, algorithms and method. *International Journal of Remote Sensing*, **25**, pp. 1893–1924.

TOUTIN, Th., CHÉNIER, R. and CARBONNEAU, Y., 2001, 3D geometric modelling of Ikonos Geo images. In *ISPRS Joint Workshop ''High Resolution from Space''*, Hannover, unpaginated CD-ROM.

USGS, 2005, SRTM DTED. US Geological Survey; http://edc.usgs.gov/products/elevation/srtmdted.html (accessed 15 June 2005).

WELCH, R. and MARKO, W., 1981, Cartographic potential of spacecraft line-array camera system: stereosat. *Photogrammetric Engineering and Remote Sensing*, **47**, pp. 1173–1185.

WERNER, M., 2001, Status of the SRTM data processing: when will the world-wide 30 m DTM data be available? In *Geo-Informationssysteme*, pp. 6–10 (Heidelberg: Herbert Wichmann/Hüthig).

ZHEN, X., HUANG, X. and KWOH, L.K., 2001, Extracting DEM from SPOT stereo images. In *20th Asian Conference on Remote Sensing*, Singapore, unpaginated CD-ROM.